ELSEVIER

Journal of Structural Geology 27 (2005) 1413–1425

JOURNAL OF STRUCTURAL GEOLOGY

www.elsevier.com/locate/jsg

A chronology of foreland deformation: ultra-violet laser $^{40}Ar/^{39}Ar$ dating of syn/late-orogenic intrusions from the Variscides of southwest Ireland

David Quinn[a,*], Patrick A. Meere[a], Jo-Anne Wartho[b]

[a] *Department of Geology, National University of Ireland, Cork, Ireland*
[b] *Department of Applied Geology, Curtin University, Bentley, WA 6102, Australia*

Received 23 June 2004; received in revised form 25 January 2005; accepted 14 February 2005
Available online 6 July 2005

Abstract

The Upper Palaeozoic sedimentary rocks of the Munster and South Munster Basins, southern Ireland, lie within the Rhenohercynian Zone of the European Variscan orogeny. This foreland region accommodated shortening during the Asturian phase of Variscan deformation at the end of the Carboniferous by the development of kilometre-scale and lower order folding, high angle reverse faulting and regional fabric development. At the southwestern extremity of the belt lies the Black Ball/White Ball Heads area of the Beara Peninsula where high-level igneous intrusions locally exhibit a close relationship with both the ductile and late brittle phases of Variscan deformation. $^{40}Ar/^{39}Ar$ ultra-violet laser analysis of phlogopite crystals from these intrusions (principally trachytic dykes) has yielded ages that, when combined with structural field relationships, help to constrain the timing of Variscan deformation in southern Ireland. These ages include 314.44 ± 1.00 Ma for a penetratively deformed lamprophric pipe on Black Ball Head, 301.98 ± 1.47–298.08 ± 0.61 Ma for dyke material associated with later stage brittle deformation and a date of 296.88 ± 0.60 Ma for an undeformed post-orogenic dyke on White Ball Head.

Keywords: Variscan deformation; $^{40}Ar/^{39}Ar$ dating; Shallow intrusions

1. Introduction

The direct isotopic dating of deformation in orogenic forelands has always been restricted by the lack of suitable syn-kinematic low-grade mineral phases associated with deformation in these peripheral tectonic settings. The mix of detrital, metamorphic and alteration phases in low-grade sedimentary rocks makes the task of dating deformation of such rocks especially difficult. Dating minerals that formed during and cooled after the peak thermal event, where available, may not necessarily represent the timing of deformation, as there can be significant temporal lags between these two events. Recent developments in geochronology of low-grade metamorphic rocks have included the Rb/Sr and $^{40}Ar/^{39}Ar$ dating of material in strain fringes that is directly related to deformation (Müller et al., 2000; Sherlock et al., 2003). These studies usually yield ages for cleavage development in a given orogenic event and are consequently limited in constraining the full temporal range of upper crustal deformation, including the late stage brittle deformation that is characteristic of foreland settings.

The indirect approach of constraining the timing of regional deformation events by dating igneous intrusions associated with this deformation is also rather limited in orogenic forelands. To date, this has essentially involved dating undeformed, orogenic collapse-related, post-tectonic granites that provide an upper age boundary to a given event (e.g. Chen et al., 1993). Ideally, the use of high-level crustal intrusions requires that these intrusions span the full temporal range of deformation. This is the case in southern Ireland where it is possible to indirectly constrain the age of Variscan deformation by dating high-level crustal intrusions that are known to be intimately associated with the complete sequence of Variscan deformation in southern Ireland. These intrusions, exposed in the Lower Palaeozoic rocks of the Black Ball/White Ball Heads area of southwest Ireland, were emplaced as pipes, dykes and sills in both ductile (folding/cleavage development) and brittle (fracturing) deformational regimes. By adopting a multifaceted approach and combining these ages with existing

* Corresponding author.
E-mail address: davequinn9@hotmail.com (D. Quinn).

0191-8141/$ - see front matter © 2005 Elsevier Ltd. All rights reserved.
doi:10.1016/j.jsg.2005.02.003

chronostratigraphical constraints and observed field structural relationships, the temporal bracketing of Variscan deformation in southern Ireland is possible.

2. Background geology of Black Ball/White Ball Heads

The Black Ball/White Ball Heads study area lies within the Lower Palaeozoic Munster Basin of southern Ireland (Fig. 1). The Munster Basin was initiated in the Middle Devonian as a major intracratonic half-graben (Williams et al., 1989). It was rapidly filled with Middle–Upper Devonian Old Red Sandstone sediments, but towards the end of the Devonian sedimentation rates dropped. Igneous activity was limited to a few isolated volcanic centres, the largest located at Lough Guitane, south of Killarney, consisting of rhyolitic lavas and volcaniclastics (Avison, 1984). A smaller fault-bound structure, the South Munster Basin, was superimposed on this largely alluvial basin, marking the start of a conformable transgression into early Carboniferous marine shallow shelf to deep basinal facies (MacCarthy, 1987). Sedimentation continued into the Namurian.

The entire Upper Palaeozoic succession of southern Ireland underwent deformation at the end of the Carboniferous and lies within the foreland Rhenohercynian Zone of the European Variscan. Cooper et al. (1986) argue that deformation took the form of early layer parallel shortening cleavage development followed by folding and accommodation thrusting. However, a significant phase of cleavage development has been locally seen to post-date folding in the Galley Head area, south Cork (Bamford and Ford, 1990). The deformation was heavily influenced by the pre-existing basin architecture, where east–west or east–north-east–west–southwest-trending basin footwall margins (as well as possible igneous bodies) formed obstacles against compression (Meere, 1995a). Bulk shortening values have been estimated at 30–40% in the west (Meere, 1995a; Bresser and Walter, 1999) and 44–52% further east (Cooper et al., 1984; Ford, 1987).

2.1. Host rock lithologies of Black Ball/White Ball Heads

The rocks of the Black Ball/White Ball Heads area consist of a sequence of Carboniferous shallow marine

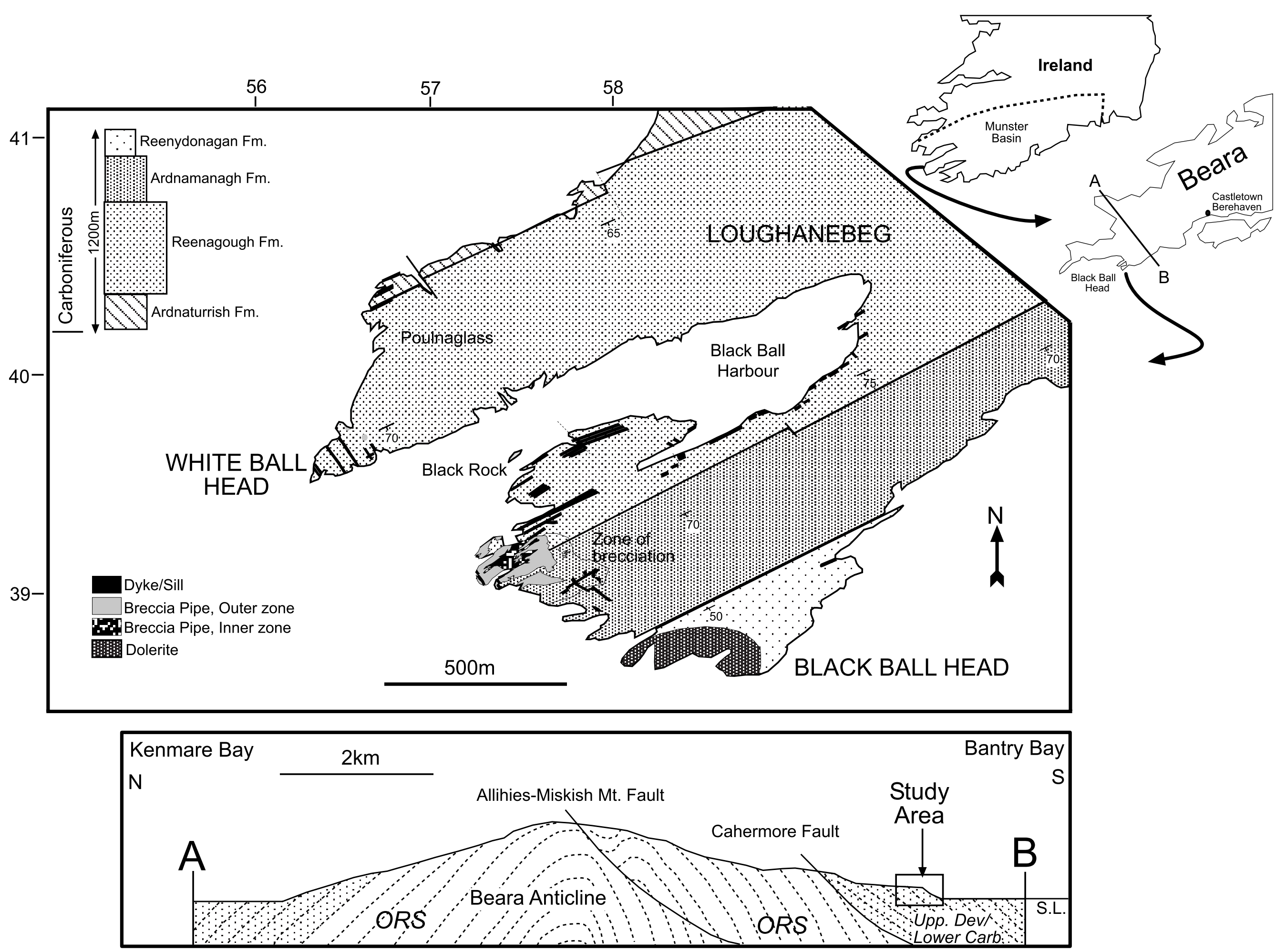

Fig. 1. Geology of the Black Ball/White Ball Heads area with simplified cross-section of the Beara Peninsula (constructed from MacCarthy, 2004).

siliclastic sediments of the Reenagough and Ardnamanagh Formations of the South Munster Basin (Williams et al., 1989) (Fig. 1). The Reenagough Formation outcrops in the White Ball Head area consist of 500 m of coarse, predominantly massive, yellow–grey sandstones that sometime display ripple surfaces and trough cross-bedding. Mudclasts, trace fossils and plant fossils are common. The general interpretation of the facies is shallow marine with shelf sand complexes or tidal sand bars (Naylor et al., 1974). The Ardnamanagh Formation outcrops in the Black Ball Head area consist largely of finely laminated siltstones and mudstones, with flaser-linsen bedding, slump sheets and channels being noted. The thickness of the unit (defined as occurring above the last massive sandstone of the Reenagough Formation and below the first limestones/calcareous mudstones of the overlying Reenydonagan Formation) is approximately 230 m. Jones (1974) interpreted this facies as representing a receding delta complex.

2.2. Igneous intrusions at Black Ball/White Ball Heads

This suite of intrusions was first documented by Kinahan (1856) and later described by Boldy (1955) and Coe (1966, 1969). More recent work focusing on geochemistry and geochronology has been published by Pracht and Kinnaird (1995, 1997). The intrusions selected for $^{40}Ar/^{39}Ar$ dating

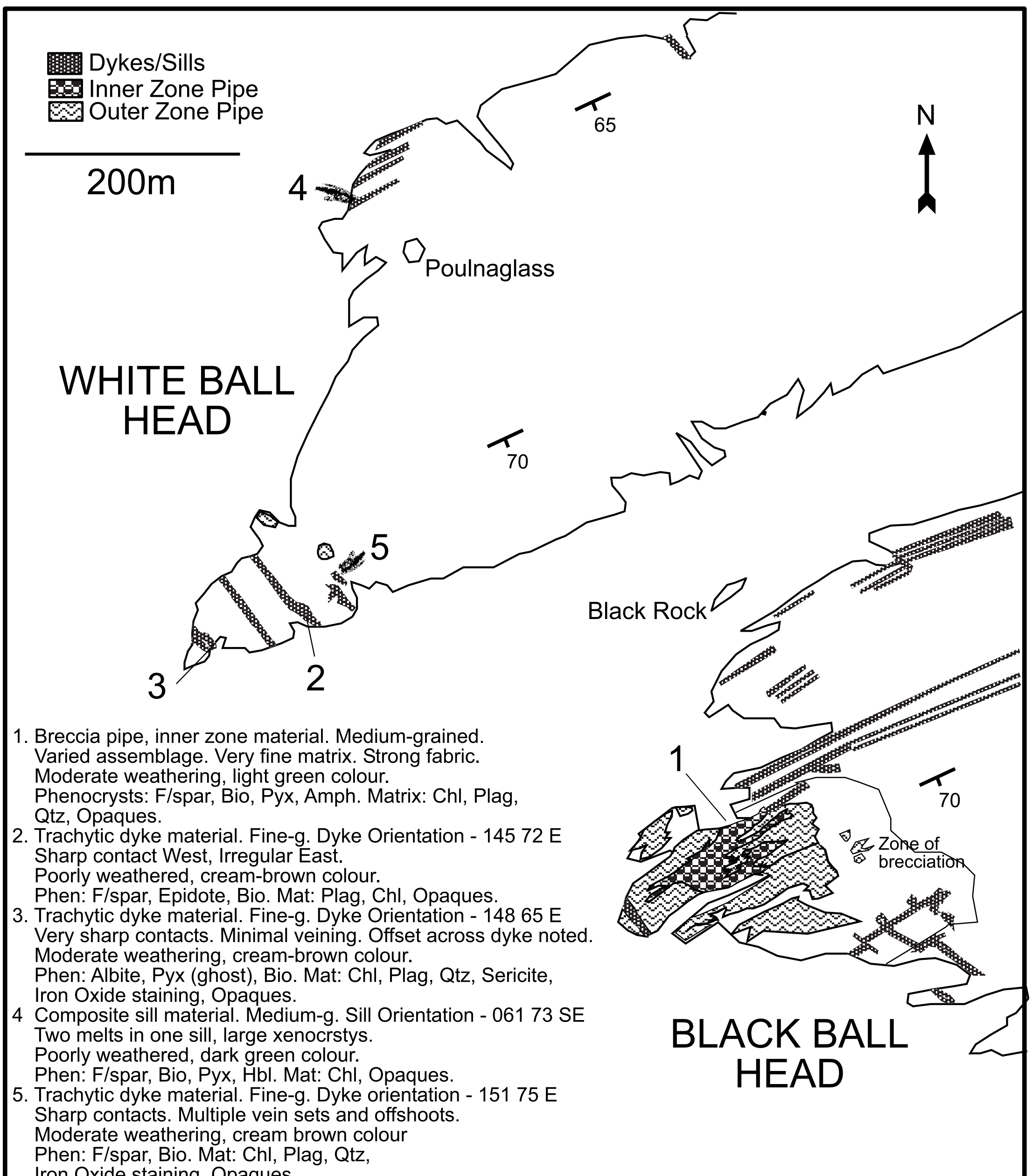

Fig. 2. Locality map for the $^{40}Ar/^{39}Ar$ geochronology samples collected from Black Ball/White Ball Heads.

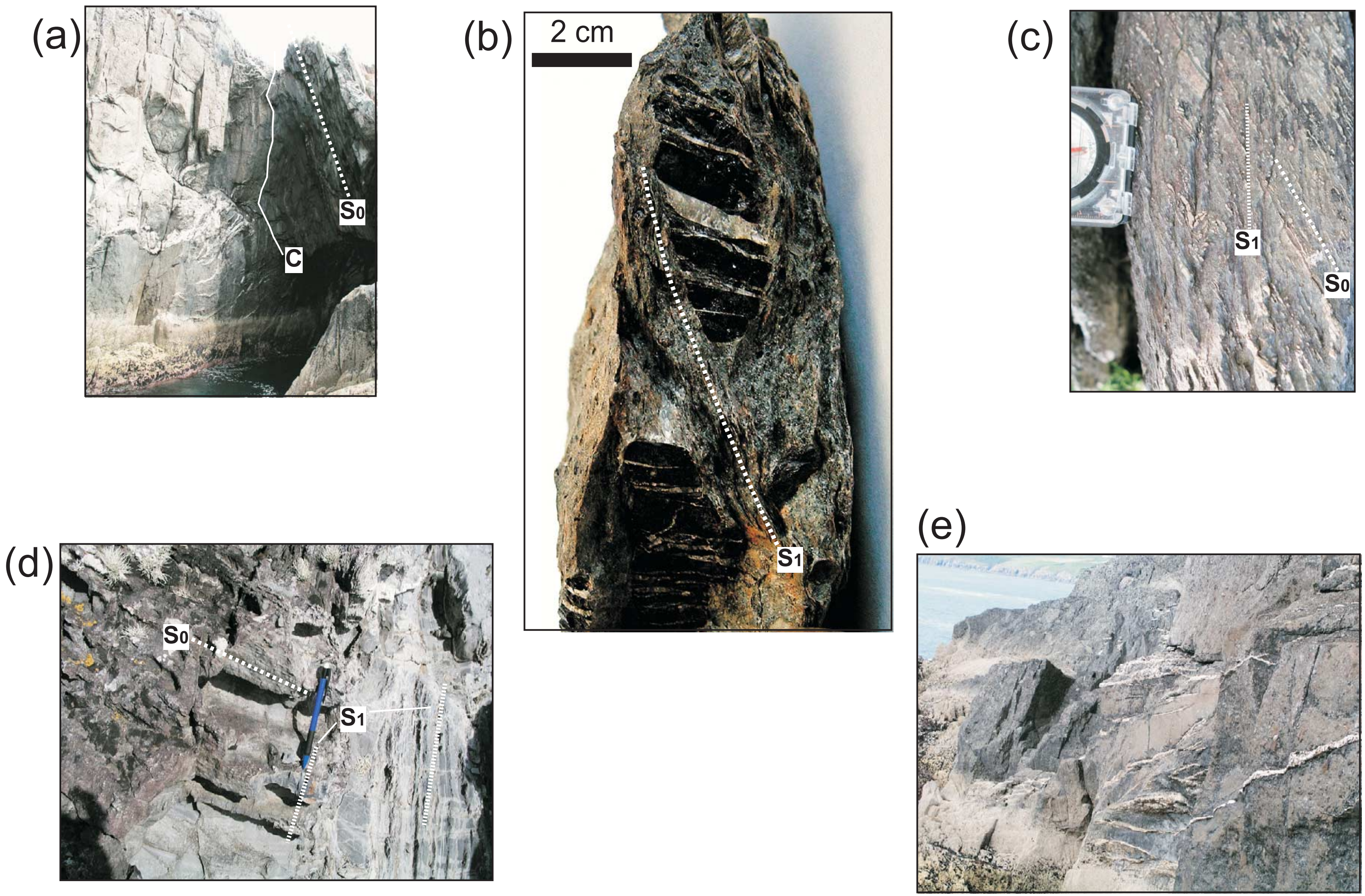

Fig. 3. Structural features on Black Ball Head. (a) Northern sub-vertical contact {C} between Black Ball Head pipe and country rock {S_0}. (b) Cleavage {S_1} wrapping around fractured megacrysts of kaersutite from the inner zone of Blackball Head pipe. (c) Bedding/cleavage relationship from Black Ball Head. (d) Marked discordance between strike of S_0 and S_1 in breccia of Black Ball Head pipe. (e) Late stage shallow dipping quartz veining from the Black Ball Head pipe.

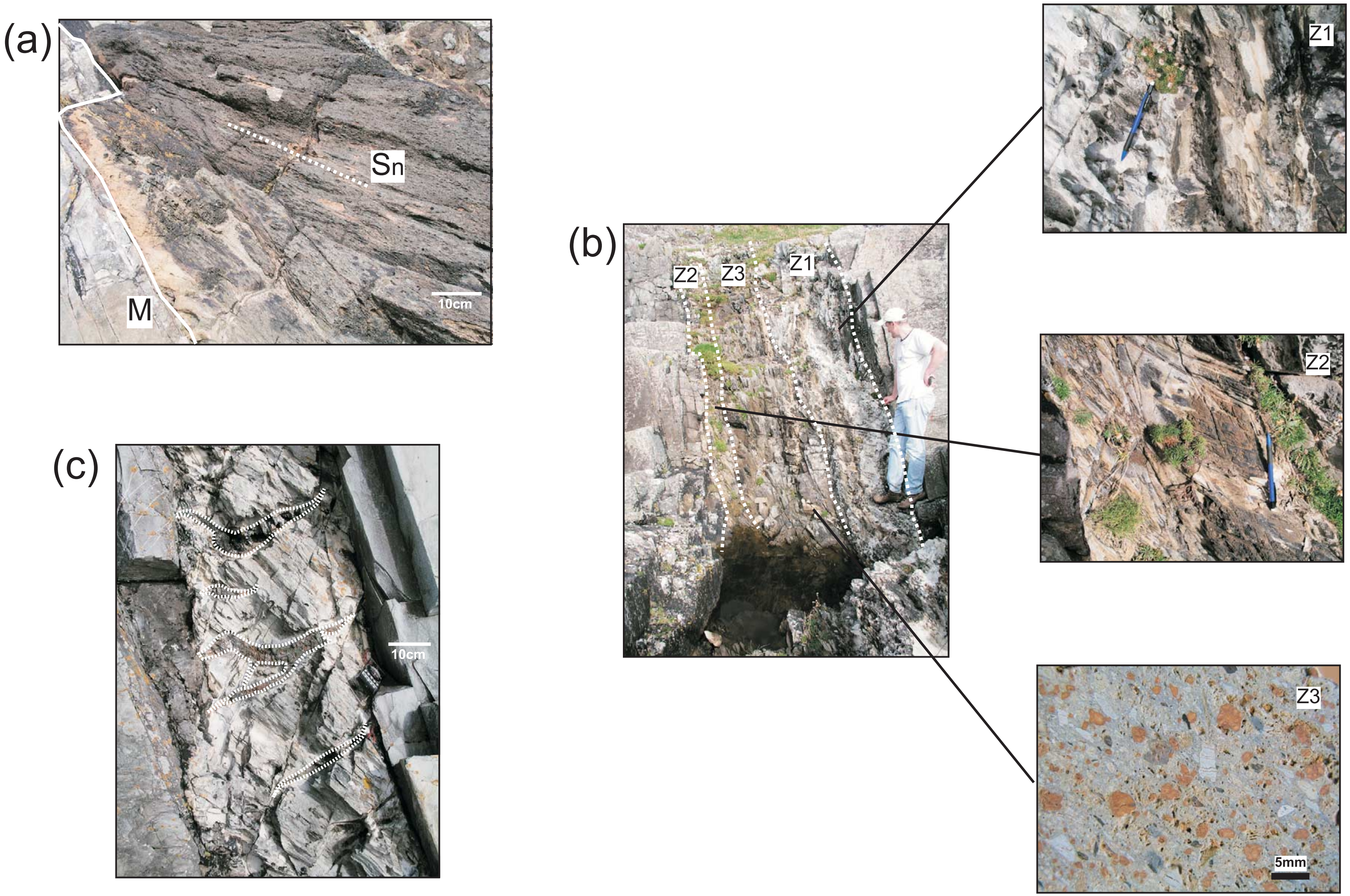

Fig. 4. Structural features on Black Ball Head. (a) Margin (*M*) of Locality 2 trachytic dyke showing well-developed fabric S_n within the dyke material. (b) Composite dyke at Locality 5 with close-ups of Zones 1–3. (c) Tension gashes developed within Zone 1 of the composite dyke at Locality 5.

are briefly described below, and the locations of the samples are shown in Fig. 2.

The suite of sills, dykes and intrusion breccia pipes are largely felsic and alkaline in composition, hosting a wide variety of phenocrysts and xenocrysts. The pipes have a lamprophric affinity, while the dykes and sills are principally trachytic. All appear to be highly altered, with chloritisation and sericitisation common. The largest pipe (roughly 150 m in diameter) is located at Black Ball Head. The margin of this pipe is highly irregular and although well exposed it is difficult to distinguish between the outer zone material and brecciated country rock. Extensive quartz veining is found particularly in the breccia material. The best exposure of the pipe/country rock contact is located on the southern flank of the pipe where it is seen to have a gently undulating geometry with a steeply dipping enveloping surface (Fig. 3a). The boundary is also seen to be steeply dipping on the northern side of the pipe where it is locally in faulted contact with the country rock. Overall, it consists of a clast-supported outer zone dominated by a wide variety of large xenoliths (up to 1.8 m long axis, and including a wide variety of host lithologies such as black shales, as well as basement granites). Most of the xenoliths show some degree of rounding indicating abrasion, and chlorite rims surround many. The inner zone assemblage consists of a diversity of xenocrysts and phenocrysts. The matrix consists of highly altered fine-grained feldspar, micas (principally phlogopite) and opaques, all of which are heavily chloritised, as well as clay minerals. Set in this extremely soft groundmass are phenocrysts of clinopyroxene (augite), feldspar (albite), phlogopite and amphibole (kaersutite megacrysts) (Fig. 3b). Also noted are pyroxenite, ilmeno-hematite and megacrysts of Ti-magnetite. Alteration rims are common and observed at field scale. This assemblage, together with the absence of garnet, orthopyroxene and olivine, represents crystallization at a depth of ca. 75 km (Pracht, 1994). While the violent nature of intrusion brecciated the host lithology, no contact metamorphism is noted.

The series of dykes outcropping at White Ball Head are highly oxidised, commonly contain vesicles, fine grained and weathered to a distinctive cream/brown colour. Replacement is widespread and makes petrological analysis difficult. The matrix consists of clay minerals, quartz and feldspar laths displaying trachytic flow texture. Feldspar phenocrysts up to 5 cm long are common, with hornblende and pyroxene occurring in minor quantities. Biotite is noted in many dykes and often displays alignment in thin section. The dykes at White Ball Head have very sharp margins as they intrude into joint planes (Fig. 4a). Chilled margins of up to 10 cm are noted, characteristic of the high level of intrusion here. At Locality 2 (Fig. 2) rafts of entrained country rock and an abundance of xenoliths are found, often rimmed by chlorite. A dyke with complex internal morphology outcrops at Locality 5 (Fig. 4b), which can broadly be divided into three distinct zones, two of which are deformed. Zone 1 is an intrusion breccia with minor entrainment of country rock and auto-brecciation is evident. A second phase of igneous material (Zone 2) is finer grained and hosts a fabric. While both east and west flanks of the intrusion display evidence of deformation, the central axis (Zone 3) is completely undeformed and fresh, with random crystal orientation and lack of fabric/shear indicators. The

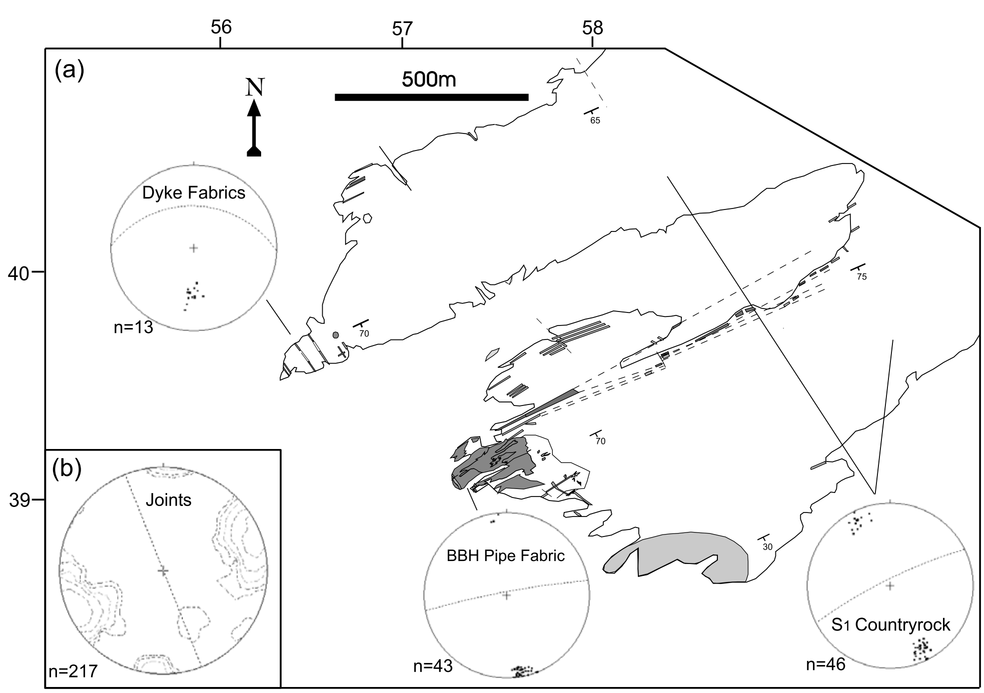

Fig. 5. (a) Fabric data and (b) joint data from the Black Ball/White Ball Heads area.

presence of this late pulse of undeformed material is extremely significant from a geochronological standpoint as it dates post-tectonism.

2.3. Structural geology of Black Ball/White Ball Heads

The study area is located on the moderately dipping southern limb of the Beara Anticlinorium, with bedding consistently dipping between 50 and 75° to the southeast (Fig. 1). The regional fold structure plunges moderately to the southwest along with lower order mesoscopic asymmetrical folding, exerting the principal structural control in the area.

Folding is associated with a penetrative cleavage that is steeply dipping and axial planar with a consistent regional strike of 065° in western Beara (Figs. 3c and 5). Some minor cleavage transections occur locally but are not systematic and are probably related to late fabric rotation out of the *X*/*Y* principal plane during fold amplification and plunge development. A widely spaced, northerly dipping fracture cleavage is locally developed on Black Ball Head. The main tectonic fabric forms a strong slaty cleavage (Fig. 3c) in the more argillaceous units (i.e. the Ardnamanagh Formation) and is usually absent in the more areneous lithologies (i.e. the Reenagough Formation).

The orientation of fabrics developed in the intrusions of the area exhibits marked deviations in orientation from the Variscan fabric in the host lithologies (Fig. 5). In the case of the main Black Ball Head pipe, a strong, steeply dipping tectonic fabric is clearly visible that shows ca. 15° clockwise discordance in strike with the Variscan fabric found in the country rock. The megacryst and xenolith assemblages are aligned parallel to the well-developed fabric, which can be seen wrapping around these components. In thin section, these elements sometimes exhibit opaque trails, indicating shearing to force alignment. This fabric orientation is internally quite consistent and overprints the marginal breccia associated with pipe emplacement (Fig. 3d). The disarticulation during pipe emplacement of host rock bedding planes within the breccia zone and subsequent overprinting of the breccia with main cleavage fabric result in a wide range of S_0/S_1 angular relationships within the breccia. Evidence of deformation on a mesoscopic scale includes the very strong penetrative cleavage in the pipe matrix with stretching and fracturing of megacrysts in the plane of cleavage (Fig. 3b). These sub-horizontal microfractures are similarly developed on a mesoscopic scale, often infilled with quartz, calcite and in some cases asbestos minerals (Coe, 1966) (Fig. 3e).

In the case of the deformed White Ball Head dykes, we see an increase in clockwise discordance between the fabric strike in the dykes and country rock to ca. 30°, with a marked decrease in dip to ca. 40–50°N (Fig. 5). There is evidence for simple shearing during fabric development across these structures with the development of quartz/chlorite filled tension gashes in a number of localities (Fig. 4c). This shearing may be related to late, relatively minor adjustments between fracture bound blocks under the influence of waning Variscan compression. In the case of the dyke at Locality 5, Zone 1, the breccia has a strong fabric with the development of tension gashes (Fig. 4b and c); the finer grained material from Zone 2 also exhibits a strong fabric while Zone 3 material is completely undeformed with a complete lack of mineral alignment or fabric development (Fig. 4b).

A systematic near-vertical joint fracture fabric overprints the Black Ball/White Ball Heads area with the dominant set striking 160° (Fig. 5b). Dykes on Black Ball Head are clearly seen to exploit pre-existing joint planes as previously noted by Coe (1966). In some places, intrusions are seen to exploit planes of differing orientation, connecting to adjacent joints along cross fractures. Dykes exploiting a fracture set other than the 160° joints rarely extend beyond a few metres. The presence of tectonic fabrics within the dyke fill of these structures is thought to reflect the low competency of this igneous material during the relatively late brittle phase of orogenic deformation.

3. Geochronology

3.1. Methodology

The freshest available samples collected from the study area with visible phlogopite crystals were prepared for in situ ultra-violet $^{40}Ar/^{39}Ar$ spot analysis. Two hundred micrometre thick sections were mounted on Lakeside cement. On arrival at Curtin University, the resin was removed from the sections and they were cleaned in an ultrasonic bath with methanol followed by deionised water. Biotite age standards Tinto B, (K–Ar age of 409.24 Ma; Rex and Guise, 1995) and HD-B1 (K–Ar age of 24.21 Ma; Hess and Lippolt, 1986) were loaded at 5 mm intervals along the Cd-shielded irradiation container to monitor the neutron flux gradient. Fast-neutron irradiation was undertaken for 20 h in the 5C position of the McMaster University Nuclear Reactor, Hamilton, Canada. The samples were returned to Curtin where they were loaded into an ultra-high vacuum laser chamber. In order to remove adsorbed atmospheric argon from the samples and chamber walls, they were baked to 120 °C. During analysis, crystals were ablated using a New Wave Research LUV 213X 4 mJ pulsed quintupled ultra-violet laser (213 nm wavelength). The gas liberated from samples was analysed in a high-sensitivity Mass Analyser Products 215-50 noble gas mass spectrometer fitted with a Balzers SEV 217 multiplier and a Nier-type source. Background blanks were run after every two analyses.

Samples were corrected for mass spectrometer discrimination and nuclear interference reactions ($^{39}Ar/^{37}Ar_{Ca}=0.00065$, $^{36}Ar/^{37}Ar_{Ca}=0.000255$, $^{40}Ar/^{39}Ar_K=0.0015$). The raw data was processed using a Microsoft Excel macro and plotted using the Isoplot macro (Ludwig, 2000). Errors quoted on the analyses and ages are 1σ, and the $^{40}Ar/^{39}Ar$ ages were calculated using the decay constant quoted by Steiger and Jäger (1977).

3.2. Results

Table 1 shows the $^{40}Ar/^{39}Ar$ data. Two additional dyke phlogopite samples (collected from White Ball Head) were unsuitable for $^{40}Ar/^{39}Ar$ analysis, as they yielded extremely low quantities of K, possibly due to extreme alteration.

During the $^{40}Ar/^{39}Ar$ analysis, high hydrocarbon/organic material concentrations were occasionally encountered in samples 2–5, which were monitored by analysing the C^{3+} peak at mass spectrometer mass 41. Contaminating hydrocarbon peaks are closely associated with every Ar isotope peak, which are fully resolved on the ^{40}Ar, ^{39}Ar and ^{38}Ar peaks, using a high-resolution (600) noble gas mass spectrometer. However, it is not possible to fully resolve the ^{37}Ar and ^{36}Ar peaks using modern available commercial and research noble gas mass spectrometers. Therefore, high levels of hydrocarbons/organics within a sample result in contamination of the ^{36}Ar peak, resulting in artificially high ^{36}Ar measurements. The ^{36}Ar concentration is very important in determining and correcting for the presence of atmospheric Ar that may be contained within a sample. An artificially high ^{36}Ar concentration results in younger than expected $^{40}Ar/^{39}Ar$ ages, and in extreme cases can yield negative ages due to overcorrection. For this reason, any $^{40}Ar/^{39}Ar$ analyses that yielded high hydrocarbon values were ignored in the calculation of the final weighted mean ages, and are not shown in Table 1. The following is a summary of $^{40}Ar/^{39}Ar$ age results.

3.2.1. Sample 1

This sample was collected from the inner zone of the intrusion breccia pipe at Black Ball Head (Fig. 2). The phlogopites yielded a range of $^{40}Ar/^{39}Ar$ ages from 295.34±13.03 to 322.20±1.61 Ma, and a weighted mean (weighted mean factor—$^{40}Ar^{*}/^{39}Ar$) $^{40}Ar/^{39}Ar$ age of 314.44±1.00 Ma (Table 1). Two $^{40}Ar/^{39}Ar$ analyses (grains 1–6 and 1–7) yielded younger ages of 261.40±12.49 and 261.38±2.56 Ma. However, these analyses had high atmospheric Ar values as shown by the lower %radiogenic ^{40}Ar ($^{40}Ar^{*}$) values of 85.6 and 78.5%, respectively (Table 1). This high atmospheric Ar component indicates probable alteration of the sample, resulting in partial loss of $^{40}Ar^{*}$ and younger than expected ages. These analyses were not included in the calculation of the mean ages.

3.2.2. Sample 2

This sample was taken from a large dyke (maximum 3 m thick) at White Ball Head (Figs. 2 and 4a). The body has sharp margins exploiting various parallel joint planes. A strong fabric is observed and alignment of large xenoliths is common. The phlogopites yielded a range of $^{40}Ar/^{39}Ar$ ages from 292.53±2.87 to 310.79±4.77 Ma, and a weighted mean $^{40}Ar/^{39}Ar$ age of 301.82±0.67 Ma (Table 1). One $^{40}Ar/^{39}Ar$ analysis (grains 2–9) yielded a younger age of 285.59±1.42 Ma, which is linked to a lower $^{40}Ar^{*}$ value of 86.3% (Table 1), indicating evidence of alteration; therefore this analysis was not included in the calculation of the mean ages.

3.2.3. Sample 3

This sample was collected from a dyke at White Ball Head ca. 0.7–1.5 m thick (Fig. 2). It outcrops between two sharp joint planes that show a few centimetres of dextral offset. It hosts a northerly dipping fabric, shown in thin section to be principally formed by alignment of biotite grains. The phlogopites yielded a range of $^{40}Ar/^{39}Ar$ ages from 284.41±6.11 to 308.29±2.46 Ma, and a weighted mean $^{40}Ar/^{39}Ar$ age of 301.98±1.47 Ma (Table 1). Two $^{40}Ar/^{39}Ar$ analyses (grains 3–8 and 3–9) yielded younger

Table 1
$^{40}Ar/^{39}Ar$ data of Samples 1–5 (1σ errors) dated from the Black Ball/White Ball Heads

	#1 phlogopite		#2 phlogopite		#3 phlogopite		#4 phlogopite		#5 phlogopite	
	Age (Ma)	+−	Age (Ma)	+−	Age (Ma)	+−	Age (Ma)	+−	Age (Ma)	+−
Grain 1	322.20	1.61	310.79	4.77	308.29	2.46	314.27	9.60	302.47	1.58
Grain 2	320.03	2.86	308.06	2.06	307.58	3.41	307.86	1.43	301.95	1.44
Grain 3	313.64	3.33	304.25	1.47	300.10	5.85	307.35	1.50	299.71	1.41
Grain 4	302.09	1.91	302.66	1.45	298.56	10.41	303.90	1.91	297.61	1.57
Grain 5	295.34	13.03	299.91	1.60	297.51	8.06	299.14	1.47	294.17	1.80
Grain 6	261.40	12.49	298.82	1.54	294.98	2.79	298.03	4.28	292.27	2.42
Grain 7	261.38	2.56	297.44	4.16	284.41	6.11	295.25	1.79	287.71	1.38
Grain 8			292.53	2.87	254.73	6.30	286.81	3.72	251.55	3.84
Grain 9			285.59	1.42	58.82	84.73	281.44	1.32	269.87	1.94
Grain 10							102.92	0.99		
Weighted mean	(Grain 1–5)		(Grain 1–8)		(Grain 1–7)		(Grain 1–9)		(Grain 1–7)	
	314.44±1.00 Ma		301.82±0.67 Ma		301.98±1.47 Ma		298.08±0.61 Ma		296.88±0.60 Ma	
Unweighted mean	311.15±9.53 Ma		301.81±5.53 Ma		298.78±7.48 Ma		299.34±9.87 Ma		296.56±5.04 Ma	

See Fig. 2 for sample localities.

ages of 254.73±6.30 and 58.82±84.73 Ma, which are linked to lower $^{40}Ar^*$ values of 74.5 and 16.8%, respectively (Table 1), indicating evidence of alteration. In addition, these two analyses also yielded very high $^{37}Ar_{Ca}/^{39}Ar_K$ ratios of 15.53 and 20.06, respectively (Table 1), indicating the degassing of a contaminating Ca-rich phase. These two analyses were not included in the calculation of the mean ages.

3.2.4. Sample 4

This sample was collected from a sill located on the northern side of White Ball Head (Fig. 2). While alignment of various elements is not obvious, a weak northerly dipping matrix fabric is noted. The phlogopites yielded a range of $^{40}Ar/^{39}Ar$ ages from 281.44±1.32 to 314.27±9.60 Ma, and a weighted mean $^{40}Ar/^{39}Ar$ age of 298.08±0.61 Ma (Table 1). One $^{40}Ar/^{39}Ar$ analysis (grains 4–10) yielded a younger age of 102.92±0.99 Ma, that is linked to a lower $^{40}Ar^*$ value of 27.6% and a higher $^{37}Ar_{Ca}/^{39}Ar_K$ ratio of 6.97 (Table 1), indicating evidence of alteration and contamination with a Ca-rich phase, therefore this analysis was not included in the calculation of the mean ages.

3.2.5. Sample 5

This sample was collected from the undeformed area (Zone 3) of the composite dyke on White Ball Head (Figs. 2 and 4b). The body occurs within sharp joint planes of similar orientation to those previously described. The phlogopites yielded a range of $^{40}Ar/^{39}Ar$ ages from 287.71±1.38 to 302.47±1.58 Ma, and a weighted mean $^{40}Ar/^{39}Ar$ age of 296.88±0.60 Ma (Table 1). Two $^{40}Ar/^{39}Ar$ analyses (grains 5–8 and 5–9) yielded younger ages of 251.55±3.84 and 269.87±1.94 Ma, that are linked to lower $^{40}Ar^*$ values of 80.2 and 87.3%, respectively (Table 1), indicating evidence of alteration, therefore these analyses were not included in the calculation of the mean ages.

4. Relationship of the igneous intrusions to deformation

The key to using the $^{40}Ar/^{39}Ar$ phlogopite ages of the high-level intrusions in the Black Ball/White Ball Heads area to constrain the timing of the Irish Variscan events is to establish the relationship these intrusions have with the full spectrum of deformation in the area, from early ductile folding/fabric development to late stage brittle fracturing. This approach presupposes that by determining the $^{40}Ar/^{39}Ar$ ages of phlogopite in these intrusions, we are in fact dating their time of emplacement. The Ar closure temperature of phlogopite is approximately 400±50 °C (e.g. Kelley and Wartho, 2000) with the error accounting for variations in grain size and cooling rate, which have an important effect on the resulting closure temperature. If the phlogopite ages are to be taken as emplacement ages the mineral have to have passed through the Ar closure temperature range during emplacement. In the case of the Black Ball Head pipe, Pracht and Kinnaird (1995) noted that the kaersutite megacryst assemblage in the inner zone of the pipe consisted of very large crystals showing a very homogenous composition across measured profiles. They noted a definite absence of compositional zoning that strongly suggests a single phase of relatively rapid crystal growth at depth of ca.75 km (ca. 20 kbar). The preservation of such an assemblage, with local evidence of extensive host rock brecciation, points to rapid emplacement of the pipe. The homogeneity and similarity in composition of the dyke and sill material on White Ball Head, as well as the presence of chilled margins and vesiculation, also suggest these intrusive events were rapid rather than protracted.

A second factor that would prevent the phlogopites in the intrusives from dropping below their Ar closure temperature during emplacement would be the background temperature of the host lithologies at the time of emplacement. Meere (1995b), in a combined illite crystallinity/fluid inclusion study of the Upper Devonian rocks of SW Ireland concluded that the regional metamorphic grade falls within the lower epizone of the greenschist facies, with peak temperatures not exceeding 325 °C. He argued that the peak thermal event was associated with high geothermal gradients due to crustal stretching during Munster Basin development. Blackmore (1995), in a vitrinite reflectance study, also concluded that the rocks of SW Ireland did not exceed epizone conditions during the peak thermal event. No thermal maturation study carried out to date indicates peak temperature in excess of 325 °C (e.g. Price, 1986; Clayton, 1989; Jones, 1992). Therefore, the conclusion can be drawn that cooling of the upper crustal intrusives in Black Ball/White Ball Head to the ambient background temperatures of the host lithologies would allow the Ar closure temperature of phlogopite (400±50 °C) to be crossed rapidly.

The chronology of structural events seen in the Black Ball/White Ball Heads area outlined in Fig. 6 is as follows:

1. Deformation is initiated with the onset of large-scale folding and bed rotation. There is no evidence in the Black Ball Head area of significant early stage layer parallel shortening fabric development. As the youngest sediments in the area consist of Namurian foreland basin turbidites, this switch to local crustal compression must have occurred during or after the Namurian.
2. The current, steeply dipping orientation of the main Black Ball Head pipe and associated brecciation of the country rocks dipping 70°S implies that it has not undergone a large component of active rotation due to Variscan folding. While passive rotation due to cleavage development tend to counteract active rotation, the bulk shortening values need to be very high to completely counteract the 70° of active rotation. Therefore, folding had to be underway before the intrusion of the pipe, i.e. the initiation of deformation pre-dated its emplacement and cooling at 314.44±1.00 Ma (Sample 1).

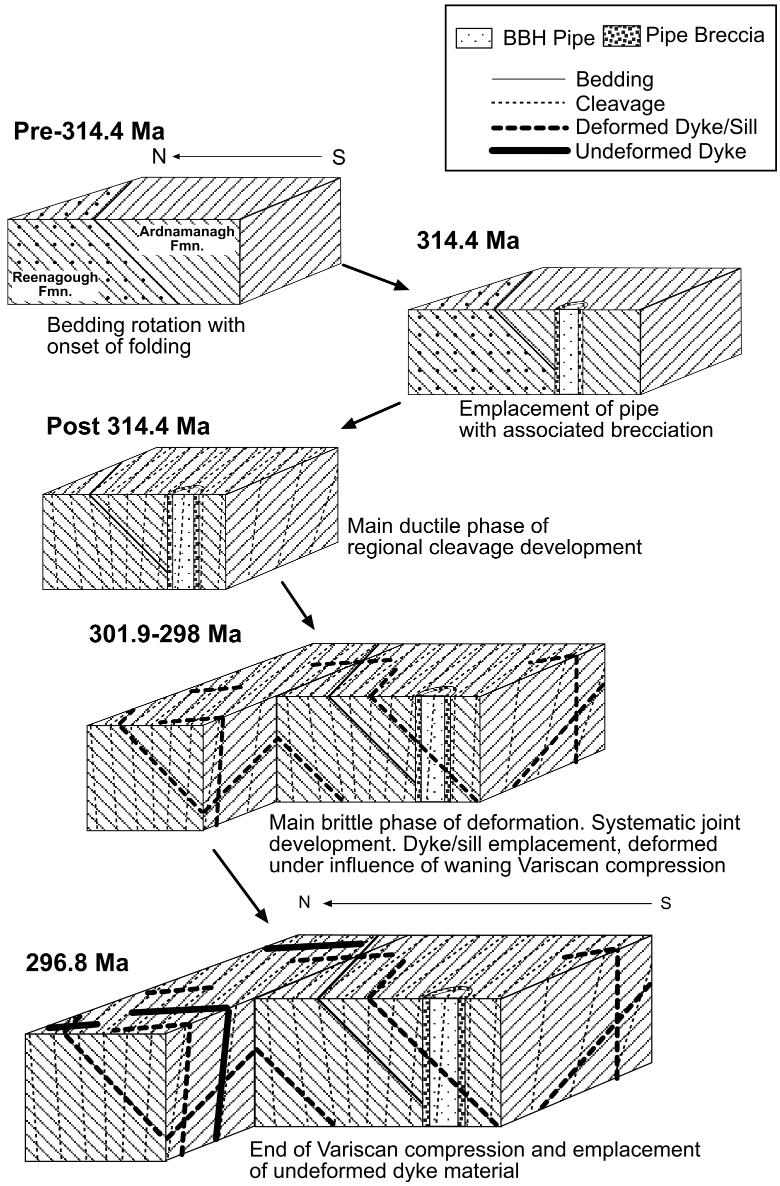

Fig. 6. Schematic block diagrams illustrating the sequence of Variscan events on Black Ball/White Ball Heads.

3. The relatively late stage development of the principal tectonic fabric is demonstrated by the variable S_0/S_1 relationships seen in the pipe breccia, with the fabric overprinting and post-dating the pipe. The consistent strike and, more importantly, uniformly high dip of the fabric seen right across the Irish Variscan, further support the notion that the fabric was not significantly rotated during folding and effectively post-dates this event. The development of an axial planar fabric can be seen as an alternative strain mechanism due to the locking-up and cessation of fold amplification. Bamford and Ford (1990) also noted significant post folding cleavage development in the Galley Head area, on the southern Irish coast.
4. The development of the systematic brittle fracture fabric, dyke emplacement and deformation mark the development of the dominant fracture set observed in the Black Ball/White Ball Heads area. It represents late-stage brittle deformation probably associated with regional uplift, but still under the influence of Variscan compression. These fractures are exploited by a series of dykes, best exposed on White Ball Head. The dyke material has been deformed with the development of a fabric dipping moderately to the north. The orientation of this fabric is probably associated with the increasing influence of gravity in the upper crustal stress field (overburden), combined with a small component of simple shear due to differential block movements across the dykes.
5. The emplacement of the final undeformed dyke material at 296.88 ± 0.60 Ma (Sample 5) delimits the upper time limit for Variscan deformation in southern Ireland.

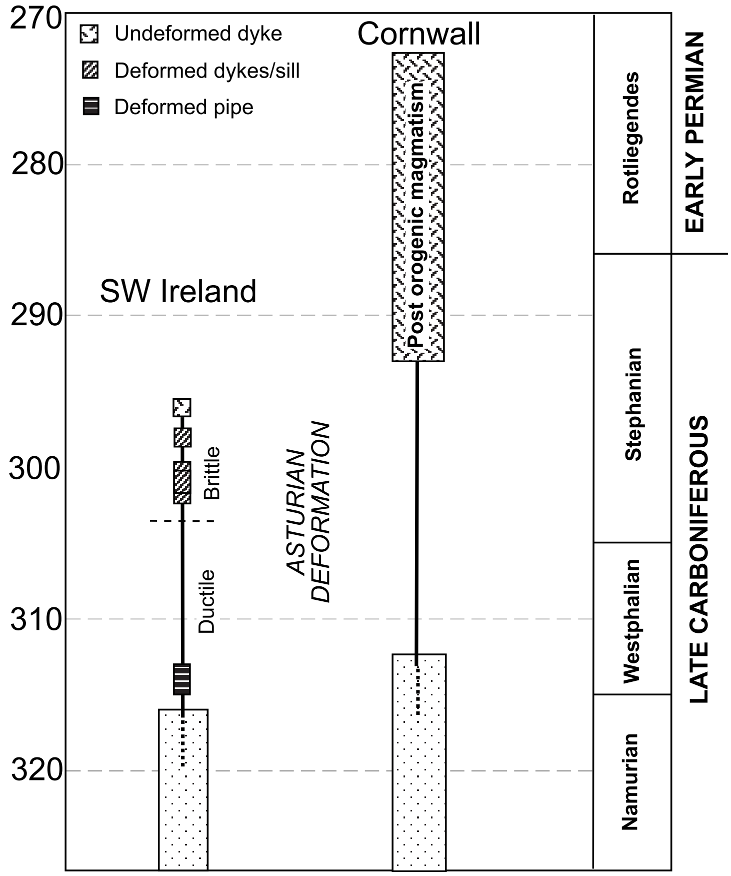

Fig. 7. Chronology of late Variscan events for southern Ireland and Cornwall.

5. Discussion

The existing age constraints for the Irish Variscan event, positioned on the northern external margin of the European Variscides, are poor. This marginal tectonic setting results in the area being only affected by the last (Asturian) phase of deformation. Pracht (1994) obtained a Rb/Sr mineral isochron age of 336±28 Ma for the deformed Black Ball Head pipe using kaersutite amphiboles and a phlogopite sample. Recently Pracht and Timmerman (2004) made reference to a revised $^{40}Ar/^{39}Ar$ (amphibole) plateau age of 318±3 Ma (2σ) for the pipe, which is interpreted to be the age of crystallisation and emplacement. While this age seems plausible and is close to that obtained in this study (314.44±1.00 Ma), it should be noted that the rapid rate of ascension means that complete degassing of the large amphiboles may not have occurred (assuming crystallisation at approximately 75 km), hence yielding an older age. The earlier studies also ignore the steeply dipping orientation of the pipe and host country rock and the implication it has for timing with respect to folding, i.e. folding must have already been underway before pipe emplacement. The Namurian and Westphalian-B sedimentary sequences of southern Ireland are all folded with local cleavage development (Nevill, 1972; Meere, 1992). Deposition of these sediments is believed to be due to lithospheric down warping as a result of a tectonically thickened crust to the south, representing a classic shallowing up foreland basin sequence. It is therefore reasonable to assume that crustal scale deformation was underway by the Namurian at the earliest in this area (Sudetian deformation is recognized earlier (Viséan) in more proximal areas of the Rhenohercynian but did not migrate northwards to this marginal zone until the Namurian, e.g. Warr, 2000).

Dating the cessation of upper crustal compression associated with a given orogeny can be quite problematic. The bulk of work constraining the end of the European Variscan is based on dating post-orogenic granites or the cooling ages of metamorphic rocks (e.g. Dallmeyer et al., 1997). Dykes have been applied to this type of problem (e.g. Wahlgren et al., 1996), but their use (and that of pipes and sills) is limited, particularly in foreland basins. The end of the orogeny in Britain is constrained by the dating of post-tectonic granites in Cornwall. The oldest of these, the Carnmenellis Granite, yields a U–Pb monazite age of 293.1±1.3 Ma (Chen et al., 1993). The end of Variscan compression in the mainland Rhenohercynian fold belt is marked by undeformed, post-tectonic gabbros and leucogranites in the Harz Mountains, central Germany. These igneous bodies were dated by Baumann et al. (1991) using the U–Pb (zircon) technique and returned dates between 293 and 297 Ma. Similar ages are recorded in the granitoids of the Mid-German Crystalline High (Anthes and Reischmann, 2001). The dating of the undeformed dyke material from Black Ball Head in this study is the first absolute age for the termination of Variscan deformation in southern Ireland. It is interesting to note that the $^{40}Ar/^{39}Ar$ phlogopite age of 296.88 ± 0.60 Ma for the Irish post-tectonic intrusive is similar to the age of the Cornish granite and the Harz suite, indicating that the end of the orogeny was a broadly synchronous event across north-west Europe (Fig. 7).

Acknowledgements

The $^{40}Ar/^{39}Ar$ data presented in this study were acquired at the Western Australian Argon Isotope Facility, operated by a consortium consisting of Curtin University and the University of Western Australia. The authors wish to thank Dr Martin Timmerman and Dr Jean Louise Mansy for their constructive reviews, and Prof. Joao Hippertt for all his help handling the manuscript.

References

Anthes, G., Reischmann, T., 2001. Timing of granitoid magmatism in the eastern mid-German crystalline rise. Journal of Geodynamics 31, 119–143.

Avison, M., 1984. Contemporaneous faulting and the eruption and preservation of the Lough Guitane Volcanic Complex, Co. Kerry. Journal of the Geological Society, London 141, 501–510.

Bamford, M.L.F., Ford, M., 1990. Flexural shear in a periclinal fold from the Irish Variscides. Journal of Structural Geology 12, 59–67.

Baumann, A., Grauert, B., Mecklenburg, S., Vinx, R., 1991. Isotope age determinations of crystalline rocks of the Upper Harz Mountains, Germany. Geologische Rundschau 80, 669–690.

Blackmore, R., 1995. Low grade metamorphism in the Upper Palaeozoic Munster Basin, southern Ireland. Irish Journal of Earth Sciences 14, 115–133.

Boldy, G.D.J., 1955. The petrology of the igneous rocks near Castletownbere, West Cork, and the tectonic relationships with the Amorican Orogeny in South-West Ireland. MSc Thesis. University Dublin.

Bresser, G., Walter, R., 1999. A new structural model for the SW Irish Variscides: the Variscan front of the NW European Rhenohercynian. Tectonophysics 309, 197–209.

Chen, Y., Hodgson, M.J., Bromley, A.V., Clark, A.H., Farrar, E., Wateneys, H.A.H.P., 1993. Diachronous and independent histories of plutonism and mineralization in the Cornubian Batholith, southwest England. Journal of the Geological Society, London 150, 1183–1191.

Clayton, G., 1989. Vitrinite reflectance data from the Kinsale Harbour—Old Head of Kinsale area, southern Ireland, and its bearing on the interpretation of the Munster Basin. Journal of the Geological Society, London 146, 611–616.

Coe, K., 1966. Intrusive tuffs in West Cork, Ireland. Quarterly Journal of the Geological Society, London 122, 1–28.

Coe, K., 1969. The geology of the minor intrusions of West Cork, Ireland. Proceedings of the Geologists' Association 80, 441–457.

Cooper, M.A., Collins, D.A., Ford, M., Murphy, F.X., Trayner, P.M., O'Sullivan, M.J., 1984. Structural style, shortening estimates and the thrust front of the Irish Variscides. In: Hutton, D.H.W., Sanderson, D.J. (Eds.), Variscan Tectonics of the North Atlantic Region Special Publication, 14. Geological Society of London, London, pp. 167–175.

Cooper, M.A., Collins, D.A., Ford, M., Murphy, F.X., Trayner, P.M., O'Sullivan, M.J., 1986. Structural evolution of the Irish Variscides. Journal of the Geological Society, London 143, 53–61.

Dallmeyer, R.D., Gil Ibarguchi, J.I.q, Gutierrez Alonso, G., Farias, P., Bastida, F., Aller, J., Martinez Catalan, J.R., Arenas, R., 1997. Diachronous Variscan tectonothermal activity in the NW Iberian Massif: evidence from $^{40}Ar/^{39}Ar$ dating of regional fabrics. Tectonophysics 277, 307–337.

Ford, M., 1987. Practical application of the sequential balancing technique: an example from the Irish Variscides. Journal of the Geological Society, London 144, 885–891.

Hess, J.C., Lippolt, H.J., 1986. $^{40}Ar/^{39}Ar$ ages of tonstein and tuff sanidines: new calibration points for the improvement of the Upper Carboniferous time scale. Chemical Geology (Isotope Geoscience Section) 59, 143–154.

Jones, P.C., 1974. Marine transgressions and facies distribution in the Cork Beds (Devonian–Carboniferous) of West Cork and Kerry, Ireland. Proceedings of the Geological Association 85, 159–187.

Jones, G.L., 1992. Irish Carboniferous conodonts record maturation levels and the influence of tectonism, igneous activity and mineralization. Terra Nova 4, 238–244.

Kelley, S.P., Wartho, J.-A., 2000. Rapid kimberlite ascent and the significance of Ar–Ar ages in xenolith phlogopite. Science 289, 609–611.

Kinahan, G.H., 1856. The igneous rocks of the Bearhaven district. Journal of the Geological Society, Dublin, 154–162.

Ludwig, K.R., 2000. Decay constant errors in U–Pb concordia-intercept ages. Chemical Geology 166, 315–318.

MacCarthy, I.A.J., 1987. Transgressive facies in the South Munster Basin, Ireland. Sedimentology 34, 389–422.

MacCarthy, I.A.J., 2004. Geology of the Devonian–Carboniferous South Munster Basin, Ireland. University College Cork/National University of Ireland, Cork.

Meere, P.A., 1992. Structural and metamorphic studies of the Irish Variscides from the Killarney–Baltimore transect, SW Ireland. PhD Thesis. NUI Cork.

Meere, P.A., 1995a. The structural evolution of the western Irish Variscides: an example of obstacle tectonics? Tectonophysics 246, 97–112.

Meere, P.A., 1995b. Sub-greenschist facies metamorphism from the Variscides of south west Ireland: an example of a syn-extensional peak thermal event. Journal of the Geological Society, London 152, 511–521.

Müller, W., Aerden, D., Halliday, A.H., 2000. Isotopic dating of strain fringe increments: duration and rates of deformation in shear zones. Science 288, 2195–2198.

Naylor, D., Jones, P.C., Matthews, S.C., 1974. Facies relationships in the Upper Devonian–Lower Carboniferous of southwest Ireland and adjacent regions. Geological Journal 9, 77–95.

Nevill, W.E., 1972. Geology of Ireland. Allan Figgus, Dublin.

Pracht, M., 1994. The geology of the Beara Penninsula, Ireland. PhD Thesis. NUI Cork.

Pracht, M., Kinnaird, J.A., 1995. Mineral chemistry of megacrysts and ultramafic nodules from an undersaturated pipe at Black Ball Head, County Cork. Irish Journal of Earth Sciences 14, 47–58.

Pracht, M., Kinnaird, J.A., 1997. Carboniferous subvolcanic activity on the Beara Peninsula, SW Ireland. Geological Journal 32, 297–312.

Pracht, M., Timmerman, M.J., 2004. A late Namurian (318 Ma) $^{40}Ar/^{39}Ar$ age for kaersutite megacrysts from the Black Ball Head diatreme: an age limit for the Variscan deformation in SW Ireland. Irish Journal of Earth Sciences 22, 33–43.

Price, C.A., 1986. Geology of the Iveragh Peninsula incorporating a remote sensing lineament study. PhD Thesis. NUI Dublin.

Rex, D.C., Guise, P.G., 1995. Evaluation of argon standards with special emphasis on time scale measurements. In: Odin, G.S. (Ed.), Phanerozoic Time Scale Bulletin Liaison of Information IUGS Subcommission on Geochronology, 13, pp. 21–23.

Sherlock, S., Kelley, S.P., Zalasiewicz, J., Evans, D.I., Merriman, R.J., Kemp, S.J., 2003. Precise dating of low temperature deformation: strain-fringe analysis by ^{40}Ar–^{39}Ar laser microprobe. Geology 31, 219–222.

Steiger, R.J., Jäger, E., 1977. Subcommission on geochronology: convention on the use of decay constants in geo- and cosmochronology. Earth and Planetary Science Letters 36, 359–362.

Wahlgren, C.H., Heaman, L.M., Kamo, S., Ingavld, E., 1996. U–Pb baddeleyite dating of dolerite dykes in the eastern part of the Sveconorwegian orogen, south-central Sweden. Precambrian Research 79, 227–237.

Warr, L.N., 2000. The Variscan Orogeny: the welding of Pangaea. In: Woodcock, N.H., Strahan, R.A. (Eds.), Geological History of Britain and Ireland. Blackwell Science, Cambridge, pp. 271–294.

Williams, E.A., Bamford, M.L.F., Cooper, M.A., Edwards, H.E., Ford, M., Grant, G.G., MacCarthy, I.A.J., McAfee, A.M., O'Sullivan, M.J., 1989. Tectonic controls and sedimentary response in the Devonian–Carboniferous Munster Basin, southwest Ireland. In: Arturton, R.S., Gutteridge, P., Nolan, S.C. (Eds.), The Role of Tectonics in Devonian and Carboniferous sedimentation in the British Isles Special Publication of the Yorkshire Geological Society, 6, pp. 123–141.